Published in final edited form as:
Immunity. 2012 September 21; 37(3): 535–548. doi:10.1016/j.immuni.2012.06.015.

Oxysterol gradient generation by lymphoid stromal cells guides activated B cell movement during humoral responses

Tangsheng Yi[1], **Xiaoming Wang**[1], **Lisa M. Kelly**[1], **Jinping An**[1], **Ying Xu**[1], **Andreas W. Sailer**[2], **Jan-Ake Gustafsson**[3], **David W. Russel**[4], and **Jason G. Cyster**[1]

[1]Howard Hughes Medical Institute and Department of Microbiology and Immunology, University of California, San Francisco, CA 94143 [2]Developmental & Molecular Pathways, Novartis Institutes for BioMedical Research, 4056 Basel, Switzerland [3]Department of Biology and Biochemistry, University of Houston [4]Department of Molecular Genetics, University of Texas Southwestern Medical Center, TX 75390

Summary

7α,25-dihydroxycholesterol (7α,25-OHC) is a ligand for the G-protein coupled receptor EBI2 (GPR183); however, the cellular sources of this oxysterol are undefined. 7α,25-OHC is synthesized from cholesterol by the stepwise actions of two enzymes, CH25H and CYP7B1, and is metabolized to a 3-oxo derivative by HSD3B7. We show that all three enzymes control EBI2-ligand concentration in lymphoid tissues. Lymphoid stromal cells are the main CH25H and CYP7B1-expressing cells required for positioning of B cells and they also mediate 7α,25-OHC inactivation. CH25H and CYP7B1 are abundant at the follicle perimeter whereas CH25H expression by follicular dendritic cells is repressed. CYP7B1-, CH25H- and HSD3B7-deficiencies each result in defective T-cell dependent plasma cell responses. These findings establish that CYP7B1 and HSD3B7, as well as CH25H, have essential roles in controlling oxysterol production in lymphoid tissues and they suggest that differential enzyme expression in stromal cell subsets establishes 7α,25-OHC gradients required for B cell responses.

Introduction

In order to mount a rapid and efficient antibody response, B cells undergo a series of dynamic movements within secondary lymphoid organs (Cyster, 2010). Naïve B cells express the chemokine receptor CXCR5 and are attracted into follicles by this receptor's ligand, CXCL13, which is made by stromal cells distributed throughout the follicle. After encountering antigen, activated B cells upregulate CCR7 and move within 6 hours to the B zone-T zone (B-T) boundary of the follicle in response to T zone-expressed CCR7 ligand, CCL21. There they interact with cognate T helper cells, and subsequently the T cell primed-

Address correspondence to: Jason G. Cyster: Jason.Cyster@ucsf.edu; phone (415) 502-6427; Fax (415) 502-8424.

Supplemental Information
Supplemental Information includes supplemental experimental procedures and 7 figures.

Competing financial interests
A.W.S is a current employee of Norvartis and holds stock and stock options in Norvartis company.

B cells down regulate CCR7 and relocate to interfollicular and outer follicular regions for further clonal expansion prior to their differentiation into short-lived antibody-secreting plasma cells or germinal center (GC) B cells (Coffey et al., 2009; Cyster, 2010; Kerfoot et al., 2011; Kitano et al., 2011). EBI2, a G protein-coupled receptor, guides B cell movement along the B-T boundary and later to interfollicular and outer follicular regions (Gatto et al., 2009; Gatto et al., 2011; Kelly et al., 2011; Pereira et al., 2009). The absence of EBI2 from B cells results in their premature accumulation in the center of the follicle and diminished T cell-dependent plasma cell differentiation (Gatto et al., 2009; Pereira et al., 2009).

7α,25-dihydroxycholesterol (7α,25-OHC) was recently identified by classic analytical methods as a high affinity ligand for EBI2 (Hannedouche et al., 2011; Liu et al., 2011). 7α,25-OHC was previously identified as an intermediate in the alternate pathway of hepatic bile acid synthesis (Russell, 2003). The conversion of cholesterol into bile acids is accomplished in the liver through two multi-enzyme pathways, commonly referred to as the classic and alternate pathways of bile acid synthesis. Studies in gene-deficient mice revealed that the essential requirement for bile acids can be met through either of the two pathways and thus that they serve compensatory roles in hepatic lipid metabolism (Russell, 2003). 7α,25-OHC is synthesized from cholesterol by CH25H mediated hydroxylation at the 25 position, followed by CYP7B1-mediated hydroxylation at the 7α position (Russell, 2003) (Fig. 1A). Unexpectedly for a protein that carries out a reaction related to bile acid synthesis, CH25H is poorly expressed in the liver but is abundant in a number of other tissues, suggesting the enzyme may function outside the liver (Lund et al., 1998; Russell, 2003). Recent studies have shown the CH25H is highly expressed in activated macrophages (Bauman et al., 2009; Diczfalusy et al., 2009; Park and Scott, 2010; Zou et al., 2011). Genetic deficiency in CH25H is shown to cause a loss of EBI2-ligand generation in lymphoid organs (Hannedouche et al., 2011). While macrophages are considered the most likely cells acting in lymphoid tissues to carry out the 25-hydroxylation reaction needed to generate EBI2 ligand (Hannedouche et al., 2011; Liu et al., 2011), their role in this process was not tested.

CYP7B1, a member of the cytochrome P450 enzyme family, is abundant in liver but *Cyp7b1* transcripts are also detected in a number of extrahepatic tissues (Stiles et al., 2009). In the kidney, CYP7B1 may contribute to de novo sterol synthesis (Li-Hawkins et al., 2000), and in the reproductive tract, the enzyme has a role in metabolizing androgens (Omoto et al., 2005). In a recent report, treatment with the non-specific cytochrome P450 inhibitor, clotramizole, reduced 7α,25-OHC in mouse spleen (Liu et al., 2011). This study provides support for CYP7B1 functioning in 7α,25-OHC generation in the spleen but indirect effects of the drug could not be excluded. Moreover, the cell types involved in 7α,25-OHC generation were not determined.

Hydroxylated sterols are further metabolized to 3-oxo, Δ^4 intermediates during the process of bile acid synthesis by a microsomal 3β-hydroxy-Δ^5-C_{27} steroid oxidoreductase (HSD3B7) (Russell, 2003) (Fig. 1A). This enzyme catalyzes isomerization of the double bond from the 5 to the 4 position and the oxidation of the 3β-hydroxyl to a 3-oxo group (Russell, 2003). HSD3B7 only acts on C_{27} sterols with a 7α-hydroxyl group. Loss of HSD3B7 blocks the synthesis of the major biologically active forms of bile acids, resulting in vitamin deficiency and cholesterol malabsorption (Shea et al., 2007). Mice with this defect can by rescued by addition of a pan-vitamin supplement to the drinking water and a bile acid (cholic acid) to the diet (Shea et al., 2007). It is not yet known if HSD3B7 acts in non-hepatic tissue on substrates such as 7α,25-OHC, nor whether 7α,25-OHC modification by HSD3B7 alters EBI2-ligand activity.

In this study we have demonstrated that CH25H, CYP7B1, and HSD3B7 constitute an extrahepatic pathway that regulates oxysterol production in lymphoid tissues. We show that

CH25H and CYP7B1 are abundantly expressed by lymphoid stromal cells and that they are required in these cells to generate the 7α,25-OHC ligand gradient that guides EBI2-mediated B cell movement. We also find that follicular dendritic cells (FDCs) are needed to allow EBI2-dependent B cell positioning within the follicle. Stromal cell HSD3B7 inactivates 7α,25-OHC, and in the absence of this enzyme, EBI2-ligand abundance is markedly increased and B cell positioning fails. HSD3B7 also functions in dendritic cells (DCs) to restrict their EBI2-ligand production. Consistent with a crucial role in generating EBI2-ligand gradients, CYP7B1, CH25H and HSD3B7 deficiencies are each associated with impaired humoral immune responses.

Results

CYP7B1 is required for generating EBI2-ligand activity

As well as being abundant in liver, CYP7B1 transcripts are present in lymphoid organs (Hannedouche et al., 2011; Li-Hawkins et al., 2000; Rose et al., 2001). To investigate whether CYP7B1 is required for EBI2-ligand generation, we prepared extracts from lymphoid tissues of CYP7B1-deficient and littermate-control mice. CYP7B1-deficient mice rely on the classic pathway of bile acid biosynthesis but are otherwise healthy and grow normally (Li-Hawkins et al., 2000; Rose et al., 2001). EBI2-ligand abundance in lymphoid tissues was assessed with a bioassay that measures the ability of tissue extracts to induce the migration of an EBI2-expressing cell line that has subnanomolar sensitivity for 7α,25-OHC in a transwell assay (Suppl. Fig. S1A&B) (Hannedouche et al., 2011; Kelly et al., 2011). Extracts from *Cyp7b1*$^{-/-}$ spleen and LNs lacked EBI2-ligand activity, whereas extracts from wild-type littermate control tissues contained readily detectable bioactivity (Fig. 1B). We also tested the sufficiency of CYP7B1 to generate EBI2-ligand in transfected cells. Overexpression of CYP7B1 in HEK293T cells did not elevate EBI2-ligand generation, but cotransfection of CH25H and CYP7B1 together achieved a strong synergistic effect in promoting ligand production (Fig. 1C). Notably, the synergistic activity of CH25H and CYP7B1 did not require coexpression in the same cells as coculturing cells that were separately overexpressing CH25H and CYP7B1 generated EBI2-ligand to a similar extent as observed for cultures of cotransfected cells (Fig. 1C). These observations suggest that 25-OHC can be transferred between cells to serve as a substrate for CYP7B1 with subsequent release of 7α,25-OHC into the culture supernatant.

To test whether CYP7B1 is required for EBI2-dependent B cell movement, we examined naïve and activated B cell positioning in *Cyp7b1*$^{-/-}$ or littermate-control recipients. Previous work has shown that at day 2 after activation by antigen and T cell interaction, B cells position to interfollicular and outer follicular regions in an EBI2-dependent manner and expression of GFP from the *Ebi2* locus in EBI2-GFP reporter mice is elevated (Coffey et al., 2009; Kerfoot et al., 2011; Kitano et al., 2011; Pereira et al., 2009). Unexpectedly, *Ebi2* transcript abundance is reduced in activated B cells at this time point (Gatto et al., 2009; Kelly et al., 2011). To clarify this situation, we used a polyclonal antiserum specific for EBI2 to demonstrate that EBI2 surface abundance was increased early after B cell activation (Fig. 1D and Suppl. Fig. S1). Surface expression remained abundant at day 2 of the T-cell dependent B cell response, though the higher background staining on *Ebi2*$^{-/-}$ B cells at this time point made it difficult to compare the expression to the earlier time points (Fig. 1D). However, by *in vitro* analysis, 7α,25-OHC chemotactic responsiveness of both 10 hour- and 2 day-activated B cells was elevated compared to naïve B cells (Fig. 1E). Using a hen egg lysozyme (HEL)-specific MD4 Ig-transgenic B cell plus ovalbumin (OVA)-specific OTII TCR transgenic T cell adoptive transfer model that allows *in situ* tracking of activated B cell distribution (Kelly et al., 2011), we found that at day 2 after HEL-OVA immunization, activated B cells in *Cyp7b1*$^{-/-}$ mice failed to move to interfollicular and outer follicular regions and instead were dispersed throughout the follicle (Fig. 1F). This distribution was

distinct from that observed for day 2-activated *Ebi2*$^{-/-}$ MD4 B cells in wild-type hosts that accumulate near the follicle center (Fig. 1F). We interpret this difference as being a consequence of the ability of the endogenous B cells in wild-type hosts to respond to EBI2-ligand, a responsiveness that allowed them preferential access to the outer follicle compared to the donor EBI2-deficient B cells. Consistent with this explanation, the presence or absence of EBI2 had no effect on day 2-activated B cell distribution in CYP7B1-deficient hosts (Fig. 1F). Finally, we examined the distribution of *Ebi2*$^{-/-}$ naïve B cells in follicles one day following transfer since these cells also show a predilection for the follicle center in wild-type hosts (Gatto et al., 2009; Pereira et al., 2009). Again, we found that this tendency to accumulate in the central follicle was lost in *Cyp7b1*$^{-/-}$ hosts (Fig. 1G). Taken together, these findings indicate that CYP7B1 is required to generate EBI2-ligand within lymphoid tissues, which in turn is needed for EBI2-dependent B cell movement to interfollicular and outer follicular regions.

HSD3B7 inactivates EBI2-ligand and is required for normal B cell positioning

HSD3B7 is abundant in liver (Schwarz et al., 2000) and expressed in lower amounts in LNs and spleen (Fig. 2A). To test for a potential role of this enzyme in regulating EBI2-ligand activity, 7α,25-OHC was incubated in chambers containing HEK293T cells transfected with a vector encoding *Hsd3b7* or a control vector. Incubation with HSD3B7-expressing cells led to a complete loss of activity in the EBI2 bioassay, suggesting that isomerization of the double bond and oxidation of the 3β-hydroxyl is sufficient to inactivate receptor binding and agonism (Fig. 2B). EBI2 bioactivity in spleen extracts could also be inactivated by HSD3B7-expressing cells (Fig 2C). As an initial approach to determine whether HSD3B7 regulated EBI2-ligand abundance in vivo, we reconstituted mice with HSD3B7 or control retroviral vector-transduced BM cells. Overexpression of HSD3B7 but not the control vector in BM-derived cells reduced splenic EBI2 bioactivity (Fig. 2D), and disrupted day 2-activated B cell positioning at the outer follicle (Fig. 2E).

Having established HSD3B7 was sufficient to degrade EBI2-ligand, we next asked is this enzyme necessary for controlling EBI2-ligand abundance in lymphoid tissues? To answer this question, we compared EBI2 bioactivity in spleen and LN extracts of *Hsd3b7*$^{+/+}$ and *Hsd3b7*$^{-/-}$ mice and found more than a 5-fold elevation in the amount of activity that could be detected (Fig. 2F and Suppl. Fig. S2A). When the tissue extract was used at high concentration (1 in 2 dilution), migration was diminished (Fig. 2F). A similar loss of migration occurred in response to high concentrations of synthetic 7α,25-OHC (Suppl. Fig. S1B), likely because of receptor desensitization before cell migration had taken place. Indeed, exposure of EBI2-transduced cells and naïve B cells to synthetic 7α,25-OHC for 35 minutes decreased EBI2 surface expression (Fig. 2G). We used the sensitivity of EBI2 to ligand-mediated down-regulation as a further approach to ask whether ligand amounts were increased in the absence of HSD3B7. Splenic follicular B cells isolated from *Hsd3b7*$^{-/-}$ mice showed reduced surface EBI2 abundance compared to cells from control mice (Fig. 2H), consistent with the presence of greater amounts of interstitial 7α,25-OHC in the lymphoid tissue of mice lacking this catabolic enzyme. Lastly, we assessed EBI2-dependent positioning in *Hsd3b7*$^{-/-}$ mice. At day 2 after HEL-OVA immunization, activated MD4 B cells did not localize at the outer follicle but instead distributed evenly throughout the follicle in *Hsd3b7*$^{-/-}$ mice (Fig. 2I). Moreover, as observed in CYP7B1-deficient hosts, *Ebi2*$^{-/-}$ day 2-activated B cells and *Ebi2*$^{-/-}$ naïve B cells failed to show any preference for the follicle center in HSD3B7-deficient hosts (Fig. 2I and Suppl. Fig. S2B). Together, these results indicate that HSD3B7 both inactivates 7α,25-OHC and maintains EBI2-ligand gradients that are crucial for proper B cell movements within lymphoid tissue.

Differential CH25H and CYP7B1 expression in outer versus inner follicle

We next dissected the cellular expression of CH25H, CYP7B1, and HSD3B7 in lymphoid organs. LN cells were separated into $CD45^+$ hematopoietic cells and $CD45^-$ stromal cells, and based on CD31 and gp38 (podoplanin) staining $CD45^-$ stromal cells were further divided into: $gp38^+CD31^-$ fibroblastic reticular cells (FRC), $gp38^+CD31^+$ lymphatic endothelial cells (LEC), $gp38^-CD31^+$ blood endothelial cells (BEC), and $gp38^-CD31^-$ double negative cells (Link et al., 2007) (Fig. 3A). CH25H, CYP7B1, and HSD3B7 expression in $CD45^-$ stromal cells was 10–1000-fold higher than in $CD45^+$ cells, whereas EBI2 was enriched in $CD45^+$ cells (Fig. 3B). Among stromal cell populations, FRCs expressed the highest amount of CYP7B1 and also had abundant CH25H (Fig. 3C), suggesting this cell type may contribute to EBI2-ligand production. To test this possibility further, double sorted $CD45^-$ stromal cell populations were cultured for 1 day and culture supernatants tested for their ability to stimulate EBI2-dependent B cell migration. Bioactivity was readily detected in FRC cultures (Fig. 3D). The high background response of the control cells to culture supernatants from the BECs and the $gp38^-CD31^-$ DN stromal cells prevented us from assessing ligand production by these cells. FRCs include stromal cells that are distributed in both the T zone and follicular regions (Cyster et al., 2000), such as the so-called marginal reticular cells (MRC) that are present in the outer margin of the follicle (Katakai et al., 2008). MRCs express TRANCE (Tnfsf11) and a high abundance of TRANCE transcripts in our FRC preparations (Fig. 3C) confirms the presence of MRCs in these samples.

Currently there are no markers available to distinguish follicular and T zone stromal cells by flow cytometry. In an effort to compare CH25H expression between these cells we performed single cell PCR for the following set of transcripts: CXCL13, CCL21, CR1-CR2 (using a primer pair common to both isoforms), CH25H and HPRT. The success of our single cell analysis was confirmed by the finding that most $gp38^+CD31^-$ stromal cells either expressed CXCL13 or CCL21 but not both; the few cells where both were detected may correspond to cell doublets. By this analysis, high CH25H transcript abundance was detected in the majority of CXCL13 and CCL21 single expressing cells (Fig. 3E). The CR1-CR2-expressing cells were restricted to the $CXCL13^+$ stromal cell subset (Fig. 3E), consistent with their being FDCs. Importantly, the amounts of CH25H transcript detected in $CR1^+CR2^+$ cells were low compared to the amounts in many of the $CXCL13^+$ $CR1^+CR2^-$ cells (Fig. 3E). To further assess enzyme abundance in FDCs compared to other $gp38^+CD31^-$ stromal cells, we initially attempted to isolate FDCs based on CR1 surface staining but this approach was unsuccessful, perhaps due to the loss of CR1 during tissue digestion. To overcome this obstacle, we intercrossed CD21-Cre mice with Rosa26-ZsGreen mice. This approach allowed FACS isolation of $ZsGreen^{hi}$ $gp38^+CD31^-$ stromal cells and their FDC identity was confirmed by the very high CR1 expression (Fig. 3F) as well as high MFGE8 and lack of CD19 (not shown). Compared to FRCs, FDCs had significantly less CH25H transcripts and slightly higher amounts of HSD3B7 (Fig. 3F).

To further investigate CH25H, CYP7B1, and HSD3B7 expression in different lymphoid compartments, we stained splenic tissue sections with anti-IgD to identify follicles and then isolated different regions by laser capture microscopy (Fig. 3G) to compare gene expression by real-time PCR. CH25H and CYP7B1 were more abundant in the outer follicle and at the T-B boundary as compared to the inner follicle (Fig. 3H). HSD3B7 was more abundant in the T zone than in B cell follicles (Fig. 3H). Since EBI2 transcriptional downregulation is important for B cell positioning in GCs (Gatto et al., 2009; Pereira et al., 2009), we immunized mice with sheep red blood cells (SRBCs) and compared CH25H, CYP7B1, and HSD3B7 expression in outer follicle, B-T boundary, and GCs. CH25H and CYP7B1 expression were more than 10-fold higher in the outer follicle and at the B-T boundary than within GCs (Fig. 3I). Taken together, these results suggest that at the tissue compartment

level, 7α,25-OHC biosynthetic capacity is highest in outer follicular regions and at the B-T boundary and T zone, whereas degradation capacity is greatest in the T zone.

Stromal cells are an important 7α,25-OHC source for B cell positioning

To test the stromal versus hematopoietic cell contribution to the production of 7α,25-OHC and the establishment of EBI2-ligand gradients, a series of reciprocal BM chimeras were generated. We found that lack of BM-derived CH25H, CYP7B1, and HSD3B7 did not change the EBI2-ligand activity detectable in whole spleen and LN tissue extracts (Fig. 4A, B, C, and Suppl. Fig.S3A). Two days after HEL-OVA immunization, activated B cells positioned similarly at inter- and outer-follicle regardless of the presence of BM derived CH25H, CYP7B1 or HSD3B7 (Suppl. Fig. S3C). $CD169^{+}$ marginal metallophilic macrophages have been speculated to be a potential EBI2-ligand source due to their outer follicle localization and the reported high expression of CH25H by macrophages (Bauman et al., 2009; Diczfalusy et al., 2009; Hannedouche et al., 2011; Liu et al., 2011; Park and Scott, 2010; Zou et al., 2011). BM reconstitution replaces most but not the entire population of host $CD169^{+}$ macrophages (Phan et al., 2009). In order to exclude possible effects of residual host-derived $CD169^{+}$ macrophages, we reconstituted $CD169^{DTR}$ recipients (Miyake et al., 2007) with BM from *Ch25h*$^{-/-}$ mice or littermate controls. Eight weeks after reconstitution, we ablated residual host macrophages by diphtheria toxin (DTx) treatment. The efficacy of the DTx treatment was confirmed in control mice (not shown and (Muppidi et al., 2011)). Activated B cells localized similarly to outer follicular regions in DTx treated $CD169^{DTR}$ mice that had been reconstituted with *Ch25h*$^{-/-}$ or *Ch25h*$^{+/+}$ BM cells (Fig. 4D). In addition, $CD169^{DTR}$ recipients reconstituted with *Ch25h*$^{-/-}$ BM and treated with DTx were immunized with SRBC and compared for CH25H expression in outer follicle and GCs by laser capture microdissection. CH25H mRNA remained more abundant in the outer follicle and at the B-T boundary compared to the GCs (Fig. 4E). Taken together, these findings suggest that BM-derived cells are not major contributors to lymphoid tissue EBI2-ligand generation under conditions of homeostasis or during the early phases of the T cell-dependent antibody response.

In reciprocal experiments, we reconstituted each type of enzyme-deficient mouse strain or their littermate controls with wild-type BM. Reconstitution with wild-type hematopoietic cells failed to restore EBI2-ligand activity in *Ch25h*$^{-/-}$ and *Cyp7b1*$^{-/-}$ recipients to amounts detected in the littermate control mice, although some ligand was generated (~80% reduced, Fig. 4F, G and Suppl. Fig. S3B). Moreover, EBI2-ligand remained elevated in *Hsd3b7*$^{-/-}$ recipients reconstituted with wild-type BM derived cells, although the ~2–3 fold over-production was less than the ~10-fold over-production observed in complete *Hsd3b7*$^{-/-}$ mice (compare Fig. 4H and 2F). These results indicate that stromal cells are major cellular sources and sinks for EBI2-ligand in lymphoid organs, while BM-derived cells contribute to a lesser extent.

We next investigated whether stromal cell enzyme deficiencies affected B cell positioning. In *Ch25h*$^{-/-}$, *Cyp7b1*$^{-/-}$, and *Hsd3b7*$^{-/-}$ mice that had been reconstituted with wild-type BM cells, day 2-activated B cells failed to accumulate in outer follicles and instead distributed evenly throughout the follicle (Fig. 4I). Moreover, EBI2-dependent segregation of naïve B cells between inner and outer follicle of spleen, LNs and Peyer's patches was disrupted in *Ch25h*$^{-/-}$, *Cyp7b1*$^{-/-}$ and *Hsd3b7*$^{-/-}$ mice reconstituted with mixtures of wild-type and *Ebi2*$^{-/-}$ BM (Supp. Fig. S3D). Taken together, these results support the above interpretation that stromal cells are the main sources and catabolic sites of the 7α,25-OHC needed to guide B cells to interfollicular and outer follicular regions.

HSD3B7 acts intrinsically in DCs to restrict EBI2-ligand generation

In addition to guiding B cells to interfollicular and outer follicular regions 2 days after T cell-dependent activation, EBI2 is involved in localizing activated B cells prior to T cell interaction. In the absence of EBI2, 6–10 hours after antigen encounter B cells cluster near the center of the follicle-T zone interface rather than distributing along its length, and sometimes extend into the T zone itself (Kelly et al., 2011). Similar to *Ebi2*$^{-/-}$ B cells, 10 hour antigen-activated wild-type B cells failed to distribute evenly along the B-T boundary in CH25H-, CYP7B1-, and HSD3B7-deficient mice and instead tended to cluster at the center of the boundary, with some cells entering more deeply into the T zone (Fig. 5A). These data are consistent with EBI2-ligand abundance normally being greater at the tips of the interface, near interfollicular regions, than at the center of the interface. Given that CCR7 ligands are thought to be rather uniformly distributed along the interface (Okada et al., 2005), the factors causing cells to favor the central location are not yet clear. We next examined whether lack of CH25H, CYP7B1, or HSD3B7 in BM derived cells affected early-activated B cell positioning along the B-T boundary. Lack of CH25H or CYP7B1 in BM-derived cells did not affect B cell positioning along the boundary (Suppl. Fig. S4A); however, lack of HSD3B7 in BM-derived cells resulted in an increase in the extent of activated B cell positioning into the T zone (Fig. 5B and C and Suppl. Fig. S4B). In this case the cells did not extend in preferentially from the center of the B-T zone interface but gained more variable access, sometimes appearing to spread into the T zone along the length of the interface. The attraction of activated B cells into the T zone was EBI2-dependent as *Ebi2*$^{-/-}$ MD4 B cells clustered at the center of the B-T interface similarly in *Hsd3b7*$^{-/-}$ and control chimeras (Fig. 5B and C and Suppl. Fig. S4C). Total splenic DCs express many more *Hsd3b7* transcripts than T or B cells (Fig. 2A) and this expression in turn restrained DC production of EBI2-ligand, as *Hsd3b7*$^{-/-}$ splenic DCs produced ~5-fold more EBI2-ligand *in vitro* than wild-type splenic DCs (Fig. 5D). The three major splenic DC subsets all expressed HSD3B7 though expression in CD8^{+} DCs was ~3-fold higher than in the other subsets (Fig. 5E). They also expressed detectable CH25H and CYP7B1, the latter enzyme also being most abundant in CD8^{+} DCs (Fig. 5E). Culture supernatants from the sorted *Hsd3b7*$^{-/-}$ DCs showed that each subset made more EBI2 ligand than its wildtype counterpart, with *Hsd3b7*$^{-/-}$ CD8^{+} DCs generating several fold more ligand than the other subsets (Fig. 5F and Suppl. Fig. S4D). Finally, EBI2 surface expression on CD4^{+} T cells from chimeric mice lacking HSD3B7 in hematopoietic cells was reduced compared to the amounts on T cells from control BM chimeras, though not to the extent seen in *Hsd3b7*$^{-/-}$ mice (Fig. 5G). Taken together, these results suggest that HSD3B7 activity in DCs, particularly CD8^{+} DCs, restrains their production of EBI2-ligand and in so doing helps maintain the central T zone as an EBI2-ligand-low environment. However, our findings do not exclude an EBI2-ligand metabolizing role for HSD3B7 in other hematopoietic cell types.

FDCs are required for EBI2-dependent B cell segregation in the follicle

The above findings established that 7α,25-OHC biosynthetic enzymes were low in the follicle center and that CH25H transcripts were lower in FDCs compared to the majority of other lymphoid stroma cells. We recently found that when FDCs are ablated, markers of T zone stromal cells become increased inside the B cell area (Wang et al., 2011). To test whether FDCs are required to maintain EBI2-ligand gradients within the follicle, *Cd21-cre*$^{+}$ /*Rosa*^{DTR} or *Rosa*^{DTR} control mice were reconstituted with Igh^{b} *Ebi2*$^{-/-}$ BM and Igh^{a} *Ebi2*$^{+/+}$ BM cells and treated with DT two days prior to analysis (Fig. 6A). FDC ablation was confirmed by the loss of CD35 (CR1) staining at the follicle center (Fig. 6B). Following FDC ablation, ER-TR7^{+} fibroblastic reticular cells were found in increased abundance within the center of B cell areas (Fig. 6B) as previously observed (Wang et al., 2011). After FDC ablation, the segregation of naïve wild-type and EBI2-knockout B cells between the outer and inner follicle, respectively, disappeared in all lymphoid tissues examined (Fig. 6C

and Suppl. Fig. S5). FDC ablation did not affect activated B cell positioning along the B-T boundary 10 hours after HEL immunization (Fig. 6D) but it prevented activated B cells from preferentially localizing at interfollicular and outer follicular regions 48 hours after HEL-OVA immunization (Fig. 6D). Moreover, the differential in CH25H expression between the inner and outer regions of the IgD^+ B cell area within splenic white pulp cords was no longer evident (Fig. 6E). Taken together, these results indicate that FDCs are required to maintain the center of the B cell area as a region with low EBI2-ligand biosynthetic capability, and they support the conclusion that this property mediates the EBI2-dependent segregation of B cells between the inner and outer follicle.

CYP7B1, CH25H and HSD3B7 are required for mounting plasma cell responses

To test the importance of CYP7B1-mediated generation of 7α,25-OHC for mounting antibody responses, we adoptively transferred GFP transgenic HEL-specific Hy10 B cells into wild-type recipients and immunized the mice with SRBC conjugated with mutated low affinity $HEL^{2\times}$ (Paus et al., 2006). We found that antigen-specific Hy10 B cells were less abundant in *Cyp7b1*$^{-/-}$ as compared with *Cyp7b1*$^{+/-}$ mice at day 5 (Fig. 7A and B). The percentage and number of IgM, IgG1 and IgG2b plasma cells were markedly reduced in *Cyp7b1*$^{-/-}$ mice (Fig. 7A and B). Similar reductions in total HEL-specific B cells and IgM, IgG1 and IgG2b plasma cells were observed when Hy10 B cells were transferred to *Ch25h*$^{-/-}$ recipients (Fig. 7C) extending the previous finding of a reduced total plasma cell response to SRBCs in *Ch25h*$^{-/-}$ mice (Hannedouche et al., 2011). In order to determine whether the diminished responses were due to the loss of EBI2-ligand, we asked whether EBI2-deficient cells showed any difference in responsiveness in wild-type versus enzyme-deficient hosts. Mixtures of *Ebi2*$^{+/+}$ ($CD45.1^+CD45.2^+$,~20%) and *Ebi2*$^{-/-}$ ($CD45.2^+$, ~80%) Hy10 B cells were transferred into *Cyp7b1*$^{+/-}$ and *Cyp7b1*$^{-/-}$ recipients and the mice were immunized with SRBC-$HEL^{2\times}$. In the control hosts, the *Ebi2*$^{-/-}$ Hy10 B cells showed a 50–80 % reduction in the plasma cell response compared to the cotransferred *Ebi2*$^{+/+}$ Hy10 B cells (Fig. 7D and E) adding to the evidence that EBI2 has a B cell intrinsic role in supporting plasma cell responses (Gatto et al., 2009). Importantly, however, the response of *Ebi2*$^{-/-}$ and *Ebi2*$^{+/+}$ Hy10 B cells was similarly low in *Cyp7b1*$^{-/-}$ hosts, indicating that the positive influence of EBI2 on the plasma cell response was lost when the host lacked *Cyp7b1*. Very similar findings were made in *Ch25h*$^{-/-}$ hosts and in *Hsd3b7*$^{-/-}$ hosts (Fig. 7F and G). These results indicate that CYP7B1, CH25H and HSD3B7 are all required for the EBI2-dependent early B cell accumulation and plasma cell response following immunization with a T-cell dependent antigen.

Discussion

CYP7B1 and HSD3B7 are best defined for their roles in bile acid synthesis in the liver (Russell, 2003). Our studies show that these two enzymes, together with CH25H, are required in lymphoid organs for the generation of EBI2-ligand gradients that guide the movements of naïve and activated B cells. We have established that HSD3B7-mediated modification of 7α,25-OHC inactivates EBI2-ligand activity. We demonstrated that CH25H, CYP7B1, and HSD3B7 constitute a metabolic pathway that is required in lymphoid stromal cells to establish B cellguiding 7α,25-OHC gradients. We also have provided evidence that FDCs are needed to maintain an EBI2-ligand-low zone in the follicle interior and that HSD3B7 restricts EBI2-ligand production by T zone DCs.

We propose the following model for how B cell-guiding EBI2-ligand gradients are established in lymphoid tissues. CH25H and CYP7B1 are needed in radiation-resistant stromal cells, are abundantly expressed and active in $CXCL13^+$ and $CCL21^+$ FRCs but not lymphocytes, and are poorly expressed in the inner follicle compared to surrounding regions. This enzyme distribution results in more ligand production at the follicle perimeter

than at the follicle center, accounting for the propensity of EBI2^{hi} cells to be attracted to the follicle perimeter (Gatto et al., 2011; Kelly et al., 2011; Pereira et al., 2009). HSD3B7 by contrast, is present in similar amounts in the inner follicle and at the perimeter, and thus we propose that by shortening the 7α,25-OHC half-life this enzyme ensures the concentration of ligand closely mirrors the distribution of the biosynthetic enzymes. CYP7B1 and CH25H are also abundant in the T zone, but in this compartment HSD3B7 is highly expressed causing T zone 7α,25-OHC to be relatively low. As a result, ligand concentrations are most likely higher along the follicle-T zone interface than within the T zone proper. In the first hours after B cell activation, CCR7 and EBI2 are both up regulated, and B cells move to the T zone in a CCR7-dependent manner (Gatto et al., 2009; Kelly et al., 2011; Pereira et al., 2009; Reif et al., 2002); however, their propensity to remain at and distribute along the length of the B-T zone interface is promoted by the abundance of EBI2-ligand in this region. Later, after activation (~day 2), when B cells have received T cell help, they maintain high EBI2 function (Fig. 1) and CXCR5 expression but down regulate CCR7 function (Chan et al., 2009; Coffey et al., 2009; Kelly et al., 2011). As a result, these cells are less strongly attracted to the B-T zone interface and relocate to the outer follicle in an EBI2-dependent manner. A recent study suggested EBI2 transmits pro-proliferative signals to B cells (Benned-Jensen et al., 2011). We have not found 7α,25-OHC to have mitogenic effects on B cells (T.Y., L.M. and J.G.C., unpubl. obs.). Our findings of similar B cell positioning and antibody response defects in mice that are unable to make 7α,25-OHC (CH25H- and CYP7B1-deficient) and in mice that have an elevated abundance of 7α,25-OHC (HSD3B7-deficient) are most consistent with B cell EBI2 functioning principally as a guidance receptor.

More abundant CH25H and CYP7B1 expression in the outer versus inner follicle highlights the specialization of follicular stromal cells in these regions. One subset of stromal cells situated immediately beneath the marginal and subcapsular sinuses is the MRC (Katakai et al., 2008). Although there is currently no method available to isolate these cells, the abundance of the MRC marker TRANCE in our FRC preparations confirms the presence of these cells and is consistent with the possibility that they are a source of CH25H and CYP7B1. We attempted to further test whether CH25H was enriched in TRANCE^{+} stromal cells by single cell PCR but found the detection of TRANCE (Tnfsf11) by this procedure to be variable. We had similar difficulties with reproducible detection of CYP7B1 in the single cell analysis. However, the single cell approach did allow us to demonstrate lower expression of CH25H by CR1-CR2^{hi} cells than by the majority of CXCL13^{+} FRCs, in agreement with the findings for flow cytometry purified FDCs. These data are in accord with the laser capture microscopy analysis suggesting that the stromal cells at the follicle center manifest only low amounts of CH25H. We propose that the loss of EBI2 gradient information following FDC ablation occurs because of the role of FDCs in repressing FRCs within follicles. The rapid invasion or induction of follicular FRCs following FDC ablation leads to a more uniform expression of CH25H and CYP7B1 throughout the B cell area and this likely causes the loss of a gradient in 7α,25-OHC biosynthetic activity. FDCs are lymphotoxin dependent and the loss of EBI2-guided B cell segregation in follicles following lymphotoxin-blockade (Pereira et al., 2009) is also consistent with this model of EBI2-ligand maintenance by FDCs. Although FDCs express CXCL13, a finding confirmed here in the single cell PCR analysis, their ablation does not cause a reduction in CXCL13 abundance in the follicle (Wang et al., 2011). Moreover, EBI2-dependent segregation remains in *Cxcl13*$^{-/-}$ recipients (Pereira et al., 2009) and we have not observed marked differences in *Cxcl13* mRNA or protein between the inner and outer follicle (Cyster et al., 2000; Wang et al., 2011), making it unlikely that the loss of EBI2-dependent B cell segregation following FDC-ablation is due to altered CXCL13 distribution.

Previous *in vitro* and *in vivo* studies have shown the potent ability of toll-like receptors (TLR) ligands and type I interferon (IFN) signaling to induce CH25H in macrophages and DCs following exposure to innate immune stimuli (Bauman et al., 2009; Diczfalusy et al., 2009; Park and Scott, 2010; Zou et al., 2011). While we have established the essential role of stromal cells in producing and degrading EBI2-ligand in lymphoid organs to support B cell migration responses, we do not exclude the possibility that macrophages (such as marginal metallophilic or subcapsular sinus macrophages) become involved in ligand production under some inflammatory conditions.

Our findings suggest that DC production of 7α,25-OHC is normally restricted by intrinsic HSD3B7-mediated degradation. It is notable that $CD8^+$ DCs expressed more *Hsd3b7* transcripts than $CD8^-$ DCs. Within the spleen, $CD8^+$ DCs (that co-express DEC205) are abundant in the inner T zone whereas $CD8^-$ DCs are abundant in the major interfollicular regions (Steinman et al., 1997). Our studies are consistent with the possibility of this difference in HSD3B7 expression contributing to the central T zone being an EBI2-ligand low zone compared to interfollicular regions. Indeed, by promoting movement to interfollicular regions, it can be speculated that EBI2 favors encounters between B cells and $CD8^-$ DCs. We anticipate that under activation conditions leading to CH25H induction (Bauman et al., 2009; Diczfalusy et al., 2009; Park and Scott, 2010; Zou et al., 2011), DC production of 7α,25-OHC exceeds HSD3B7-mediated degradation and acts to promote new interactions between DCs and EBI2-expressing cells. Although HSD3B7 transcripts were ~10-fold more abundant in DCs than in lymphocytes, our studies do not exclude roles for hematopoietic cells other than DCs in mediating 7α,25-OHC metabolism in the T zone.

CYP7B1-deficiency causes a loss of detectable EBI2-ligand production in lymphoid organs, consistent with this being the only enzyme known to catalyze 7α-hydroxylation of 25-OHC (Russell, 2003) and with the finding of reduced 7α,25-OHC in spleens of clotramizole treated mice (Liu et al., 2011). CYP7B1 will 7α-hydroxylate 27-hydroxycholesterol to produce 7α,27-OHC, another EBI2-ligand that is about one tenth as potent as 7α,25-OHC in migration assays (Hannedouche et al., 2011; Liu et al., 2011). The loss of EBI2-ligand function in CH25Hdeficient mice, animals that retain fully the ability to synthesize 27-OHC and 7α,27-OHC, argues against a major role for 7α,27-OHC in guiding the movement of B cells in lymphoid tissues. It remains possible that 7α,27-OHC functions to control a cellular behavior not studied here.

Moreover, since both 7α,25-OHC and 7α,27-OHC are substrates for HSD3B7 (Russell, 2003), it is possible that some of the increase in EBI2-ligand detectable in the absence of this enzyme is attributable to 7α,27-OHC. Additional studies will be needed to quantify 7α, 25-OHC and 7α,27-OHC concentrations in mouse lymphoid and peripheral tissues.

Although compromised in EBI2-ligand production, CYP7B1-deficient mice have elevated circulating 25-OHC and 27-OHC (Bauman et al., 2009; Li-Hawkins et al., 2000). These oxysterols have the capacity to modulate some immune cell functions through actions on nuclear hormone receptors (Bensinger et al., 2008; Kalaany and Mangelsdorf, 2006; Villablanca et al., 2010) and to regulate IgA production (Bauman et al., 2009). Increases in these oxysterols are unlikely to account for the defective IgM and IgG plasma cell responses we describe here because EBI2-deficient B cells are equally compromised in generating plasma cells in both wild-type and CYP7B1-deficient hosts. That is, the positive influence of CYP7B1 in promoting IgM and IgG plasma cell responses appears to depend upon generation of EBI2-ligand and signaling via EBI2. Moreover, in contrast to the altered mucosal IgA responses seen in CH25H- and CYP7B1-deficient mice (Bauman et al., 2009), we have not detected altered IgA production in EBI2-deficient mice (unpubl. obs.). Further supporting the conclusion that it is the amount of EBI2-ligand that is important is the finding

of similar defects in the plasma cell response in *Ch25h*$^{-/-}$ and *Hsd3b7*$^{-/-}$ mice. An important challenge for future studies will be to elucidate whether EBI2, CH25H, CYP7B1 and HSD3B7 support B cell responses by promoting more efficient interactions between B and T cells at the B-T boundary and in interfollicular regions, or by promoting interactions between early plasmablasts and factors in interfollicular and outer follicular regions that support their growth and differentiation.

Experimental Procedure

Mice

C57BL/6NCr and C57BL/6-cBrd/cBrd/Cr (CD45.1) mice at age 7–9 weeks were from National Cancer Institute (Frederick, MD). B6.Cg-Igh^{a}Thy1^{a}Gp1^{a}/J mice, B6-Gt (ROSA)26Sor$^{tm1(HBEGF)Awai (Rosa-DTR)}$ mice, B6.Cg-Gt(ROSA)26Sor$^{tm6(CAG-Zsgreen1)Hze}$/J mice, and GFP transgenic mice (Tg(UBC-GFP)30Scha/J) were from Jackson Laboratory. *Ebi2*$^{-/-}$ mice (Pereira et al., 2009) were backcrossed to C57BL/6J for eleven generations. These mice carry an *eGfp* gene inserted in place of the Ebi2 open reading frame. *Ch25h*$^{-/-}$ mice (Bauman et al., 2009) were backcrossed ten generations to C57BL/6, *Cyp7b1*$^{-/-}$ mice were of either of two strains (Li-Hawkins et al., 2000; Rose et al., 2001) and backcrossed to C57BL/6J for five generations. *Hsd3b7*$^{-/-}$ mice were backcrossed to C57BL6/J for two generations and maintained on chow containing 0.5% cholic acid and pan-vitamin supplemented water (Shea et al., 2007). CD169^{DTR} mice (Miyake et al., 2007), B6.Tg(Cr2-Cre)3Cgn (CD21-cre) mice, HEL-specific MD4 Ig-transgenic and Hy10 mice and OVA-specific OTII TCR-transgenic mice were on a C57BL/6J background. Animals were housed in a specific pathogen-free environment in the Laboratory Animal Research Center at the University of California, San Francisco, and all experiments conformed to ethical principles and guidelines approved by the Institutional Animal Care and Use Committee.

Cell adoptive transfer and immunizations

For visualization of in situ B cell position at day 2 of the T cell-dependent response, mice were adoptively transferred with 1–10×10^{6} wild-type or *Ebi2*$^{-/-}$ MD4 splenocytes and 1–5×10^{6} wild-type OTII splenocytes. One day after cell transfer, recipients were i.p. immunized with 50 μg HEL-OVA conjugate in RIBI-based Sigma adjuvant system. To examine activated B cell distribution at 10 hours after antigen exposure, mice were given 10^{7} MD4 splenocytes the day before and were injected i.p. with 5 mg HEL in the absence of adjuvant. For antibody responses, 1×10^{5} Hy10 B cells were adoptively transferred into *Cyp7b1*$^{-/-}$, *Ch25h*$^{-/-}$, *Hsd3b7*$^{-/-}$ or littermate *Cyp7b1*$^{+/-}$ recipients. One day after cell transfer, recipients were i.p. immunized with 2×10^{8} sheep red blood cells conjugated with low affinity HEL$^{2\times}$ as described (Gatto et al., 2009).

Supplementary Material

Refer to Web version on PubMed Central for supplementary material.

Acknowledgments

We thank Robert Brink for providing HEL$^{2\times}$, Masato Tanaka for CD169^{DTR} mice, Richard Lathe for making Cyp7b1$^{+/-}$ mice available and Michael Barnes and Andrea Reboldi for comments on the manuscript. T.Y. is an Irvington postdoctoral fellow of Cancer Research Institute and J.G.C. in an Investigator of the Howard Hughes Medical Institute. This work was supported by NIH grants AI40098 and HL20948.

References

Bauman DR, Bitmansour AD, McDonald JG, Thompson BM, Liang G, Russell DW. 25-Hydroxycholesterol secreted by macrophages in response to Toll-like receptor activation suppresses immunoglobulin A production. Proc. Natl. Acad. Sci. U. S. A. 2009; 106:16764–16769. [PubMed: 19805370]

Benned-Jensen T, Smethurst C, Holst PJ, Page KR, Sauls H, Sivertsen B, Schwartz TW, Blanchard A, Jepras R, Rosenkilde MM. Ligand modulation of the Epstein-Barr virus-induced seven-transmembrane receptor EBI2: identification of a potent and efficacious inverse agonist. J. Biol. Chem. 2011; 286:29292–29302. [PubMed: 21673108]

Bensinger SJ, Bradley MN, Joseph SB, Zelcer N, Janssen EM, Hausner MA, Shih R, Parks JS, Edwards PA, Jamieson BD, Tontonoz P. LXR signaling couples sterol metabolism to proliferation in the acquired immune response. Cell. 2008; 134:97–111. [PubMed: 18614014]

Chan TD, Gatto D, Wood K, Camidge T, Basten A, Brink R. Antigen affinity controls rapid T-dependent antibody production by driving the expansion rather than the differentiation or extrafollicular migration of early plasmablasts. J. Immunol. 2009; 183:3139–3149. [PubMed: 19666691]

Coffey F, Alabyev B, Manser T. Initial clonal expansion of germinal center B cells takes place at the perimeter of follicles. Immunity. 2009; 30:599–609. [PubMed: 19303334]

Cyster JG. B cell follicles and antigen encounters of the third kind. Nat. Immunol. 2010; 11:989–996. [PubMed: 20959804]

Cyster JG, Ansel KM, Reif K, Ekland EH, Hyman PL, Tang HL, Luther SA, Ngo VN. Follicular stromal cells and lymphocyte homing to follicles. Immunol. Rev. 2000; 176:181–193. [PubMed: 11043777]

Diczfalusy U, Olofsson KE, Carlsson AM, Gong M, Golenbock DT, Rooyackers O, Flaring U, Bjorkbacka H. Marked upregulation of cholesterol 25-hydroxylase expression by lipopolysaccharide. J. Lipid Res. 2009; 50:2258–2264. [PubMed: 19502589]

Gatto D, Paus D, Basten A, Mackay CR, Brink R. Guidance of B cells by the orphan G protein-coupled receptor EBI2 shapes humoral immune responses. Immunity. 2009; 31:259–269. [PubMed: 19615922]

Gatto D, Wood K, Brink R. EBI2 operates independently of but in cooperation with CXCR5 and CCR7 to direct B cell migration and organization in follicles and the germinal center. J. Immunol. 2011; 187:4621–4628. [PubMed: 21948984]

Hannedouche S, Zhang J, Yi T, Shen W, Nguyen D, Pereira JP, Guerini D, Baumgarten BU, Roggo S, Wen B, et al. Oxysterols direct immune cell migration via EBI2. Nature. 2011; 475:524–527. [PubMed: 21796212]

Kalaany NY, Mangelsdorf DJ. LXRS and FXR: the yin and yang of cholesterol and fat metabolism. Annu. Rev. Physiol. 2006; 68:159–191. [PubMed: 16460270]

Katakai T, Suto H, Sugai M, Gonda H, Togawa A, Suematsu S, Ebisuno Y, Katagiri K, Kinashi T, Shimizu A. Organizer-like reticular stromal cell layer common to adult secondary lymphoid organs. J. Immunol. 2008; 181:6189–6200. [PubMed: 18941209]

Kelly LM, Pereira JP, Yi T, Xu Y, Cyster JG. EBI2 guides serial movements of activated B cells and ligand activity is detectable in lymphoid and non-lymphoid tissues. J. Immunol. 2011; 187:3026–3032. [PubMed: 21844396]

Kerfoot SM, Yaari G, Patel JR, Johnson KL, Gonzalez DG, Kleinstein SH, Haberman AM. Germinal center B cell and T follicular helper cell development initiates in the interfollicular zone. Immunity. 2011; 34:947–960. [PubMed: 21636295]

Kitano M, Moriyama S, Ando Y, Hikida M, Mori Y, Kurosaki T, Okada T. Bcl6 protein expression shapes pre-germinal center B cell dynamics and follicular helper T cell heterogeneity. Immunity. 2011; 34:961–972. [PubMed: 21636294]

Li-Hawkins J, Lund EG, Turley SD, Russell DW. Disruption of the oxysterol 7alpha-hydroxylase gene in mice. J. Biol. Chem. 2000; 275:16536–16542. [PubMed: 10748048]

Link A, Vogt TK, Favre S, Britschgi MR, Acha-Orbea H, Hinz B, Cyster JG, Luther SA. Fibroblastic reticular cells in lymph nodes regulate the homeostasis of naive T cells. Nat. Immunol. 2007; 8:1255–1265. [PubMed: 17893676]

Liu C, Yang XV, Wu J, Kuei C, Mani NS, Zhang L, Yu J, Sutton SW, Qin N, Banie H, et al. Oxysterols direct B-cell migration through EBI2. Nature. 2011; 475:519–523. [PubMed: 21796211]

Lund EG, Kerr TA, Sakai J, Li WP, Russell DW. cDNA cloning of mouse and human cholesterol 25-hydroxylases, polytopic membrane proteins that synthesize a potent oxysterol regulator of lipid metabolism. J. Biol. Chem. 1998; 273:34316–34327. [PubMed: 9852097]

Miyake Y, Asano K, Kaise H, Uemura M, Nakayama M, Tanaka M. Critical role of macrophages in the marginal zone in the suppression of immune responses to apoptotic cell-associated antigens. J. Clin. Invest. 2007; 117:2268–2278. [PubMed: 17657313]

Muppidi JR, Arnon TI, Bronevetsky Y, Veerapen N, Tanaka M, Besra GS, Cyster JG. Cannabinoid receptor 2 positions and retains marginal zone B cells within the splenic marginal zone. J. Exp. Med. 2011; 208:1941–1948. [PubMed: 21875957]

Okada T, Miller MJ, Parker I, Krummel MF, Neighbors M, Hartley SB, O'Garra A, Cahalan MD, Cyster JG. Antigen-engaged B cells undergo chemotaxis toward the T zone and form motile conjugates with helper T cells. PLoS Biol. 2005; 3:e150. [PubMed: 15857154]

Omoto Y, Lathe R, Warner M, Gustafsson JA. Early onset of puberty and early ovarian failure in CYP7B1 knockout mice. Proc. Natl. Acad. Sci. U. S. A. 2005; 102:2814–2819. [PubMed: 15710898]

Park K, Scott AL. Cholesterol 25-hydroxylase production by dendritic cells and macrophages is regulated by type I interferons. J. Leukoc. Biol. 2010; 88:1081–1087. [PubMed: 20699362]

Paus D, Phan TG, Chan TD, Gardam S, Basten A, Brink R. Antigen recognition strength regulates the choice between extrafollicular plasma cell and germinal center B cell differentiation. J. Exp. Med. 2006; 203:1081–1091. [PubMed: 16606676]

Pereira JP, Kelly LM, Xu Y, Cyster JG. EBI2 mediates B cell segregation between the outer and centre follicle. Nature. 2009; 460:1122–1126. [PubMed: 19597478]

Phan TG, Green JA, Gray EE, Xu Y, Cyster JG. Immune complex relay by subcapsular sinus macrophages and noncognate B cells drives antibody affinity maturation. Nat. Immunol. 2009; 10:786–793. [PubMed: 19503106]

Reif K, Ekland EH, Ohl L, Nakano H, Lipp M, Forster R, Cyster JG. Balanced responsiveness to chemoattractants from adjacent zones determines B-cell position. Nature. 2002; 416:94–99. [PubMed: 11882900]

Rose K, Allan A, Gauldie S, Stapleton G, Dobbie L, Dott K, Martin C, Wang L, Hedlund E, Seckl JR, et al. Neurosteroid hydroxylase CYP7B: vivid reporter activity in dentate gyrus of gene-targeted mice and abolition of a widespread pathway of steroid and oxysterol hydroxylation. J. Biol. Chem. 2001; 276:23937–23944. [PubMed: 11290741]

Russell DW. The enzymes, regulation, and genetics of bile acid synthesis. Annu. Rev. Biochem. 2003; 72:137–174. [PubMed: 12543708]

Schwarz M, Wright AC, Davis DL, Nazer H, Bjorkhem I, Russell DW. The bile acid synthetic gene 3beta-hydroxy-Delta(5)-C(27)-steroid oxidoreductase is mutated in progressive intrahepatic cholestasis. J. Clin. Invest. 2000; 106:1175–1184. [PubMed: 11067870]

Shea HC, Head DD, Setchell KD, Russell DW. Analysis of HSD3B7 knockout mice reveals that a 3alpha-hydroxyl stereochemistry is required for bile acid function. Proc. Natl. Acad. Sci. U. S. A. 2007; 104:11526–11533. [PubMed: 17601774]

Steinman RM, Pack M, Inaba K. Dendritic cells in the T-cell areas of lymphoid organs. Immunol. Rev. 1997; 156:25–37. [PubMed: 9176697]

Stiles AR, McDonald JG, Bauman DR, Russell DW. CYP7B1: one cytochrome P450, two human genetic diseases, and multiple physiological functions. J. Biol. Chem. 2009; 284:28485–28489. [PubMed: 19687010]

Villablanca EJ, Raccosta L, Zhou D, Fontana R, Maggioni D, Negro A, Sanvito F, Ponzoni M, Valentinis B, Bregni M, et al. Tumor-mediated liver X receptor-alpha activation inhibits CC

chemokine receptor-7 expression on dendritic cells and dampens antitumor responses. Nat. Med. 2010; 16:98–105. [PubMed: 20037595]

Wang X, Cho B, Suzuki K, Xu Y, Green JA, An J, Cyster JG. Follicular dendritic cells help establish follicle identity and promote B cell retention in germinal centers. J. Exp. Med. 2011; 208:2497–2510. [PubMed: 22042977]

Zou T, Garifulin O, Berland R, Boyartchuk VL. Listeria monocytogenes infection induces prosurvival metabolic signaling in macrophages. Infect. Immun. 2011; 79:1526–1535. [PubMed: 21263022]

Highlights

- Bile acid enzyme CYP7B1 is required for EBI2-ligand generation and B cell responses
- HSD3B7 inactivates EBI2-ligand and is required in stromal cells for gradient generation
- FDCs are required for EBI2-dependent B cell segregation in the follicle
- HSD3B7 restricts EBI2-ligand production by T zone dendritic cells

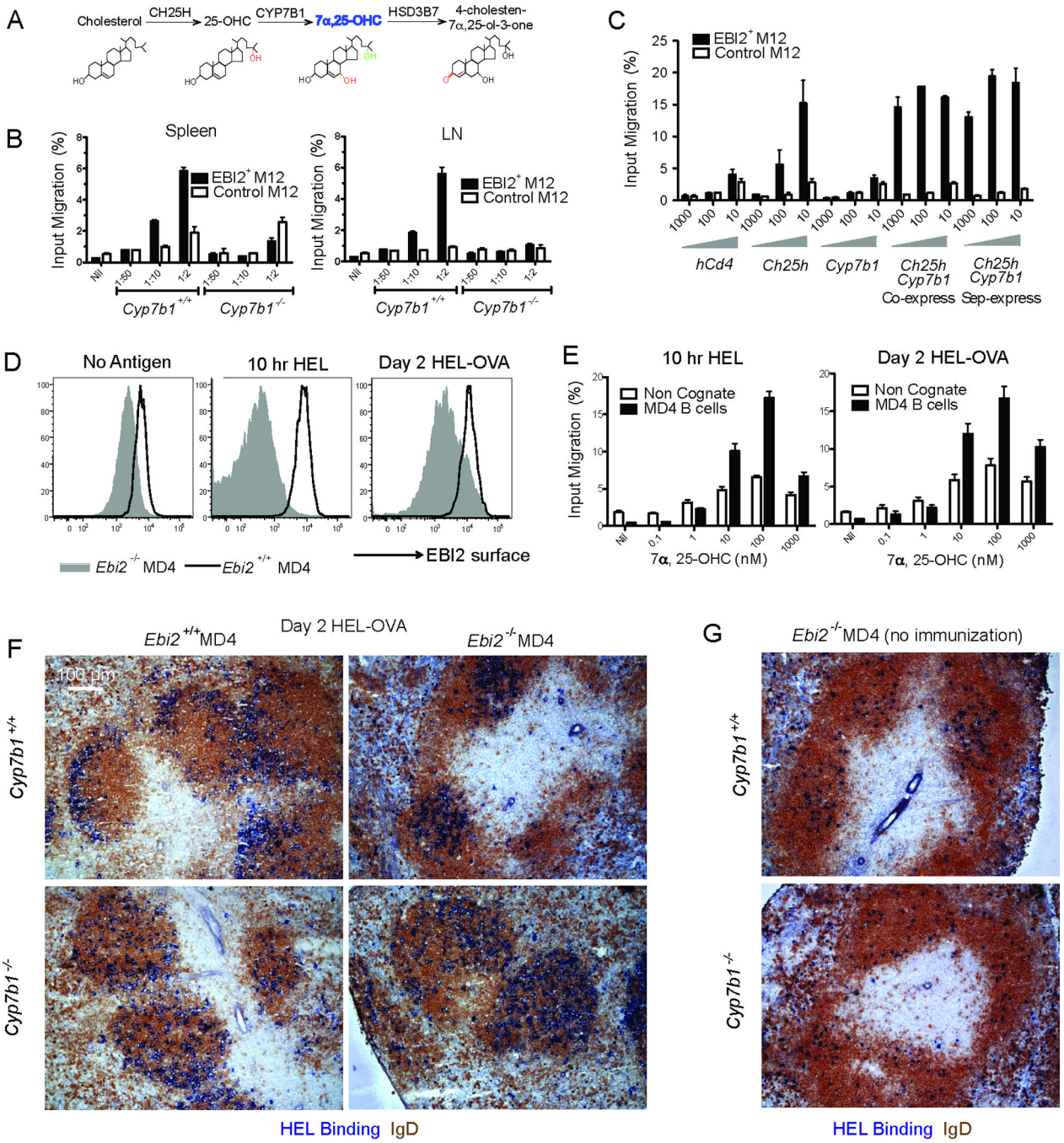

Figure 1. CYP7B1 is required for EBI2-ligand generation and activated B cell positioning

(A) Enzymatic steps catalyzed by CH25H, CYP7B1 and HSD3B7. (B) Bioassay of titrated dilutions of spleen and LN extracts from *Cyp7b1*$^{-/-}$ or wild-type animals using a reporter cell line (M12) with or without EBI2 (mean±SE, n=4 mice). (C) Bioassay of titrated dilutions of supernatant from 293T cells transfected with the empty vector (Ctrl) or vector(s) encoding CH25H, CYP7B1, CH25H plus CYP7B1 (co-express), or from a mixture of the individually transfected cells (Sep-express) (mean±SE, n=4 from 2 experiments). (D) EBI2 surface staining of *Ebi2*$^{-/-}$ or wild-type MD4 B cells 10 hr after HEL immunization or 48 hr after HEL-OVA immunization (1 representative of 3 experiments). (E) Migration of antigen-specific (MD4) B cells and non-cognate B cells from spleens of 10 hr- or 2 day-

immunized recipients (as in D) in response to 7α,25-OHC (mean±SE, 4 mice in each group, 1 representative of 2 experiments). (F,G) Spleen sections were analyzed from the indicated mice, with (F) or without (G) immune challenge. Transferred MD4 B cells were detected by HEL-binding (blue) and endogenous B cells by anti-IgD (brown). Data are representative of at least 3 independent experiments.

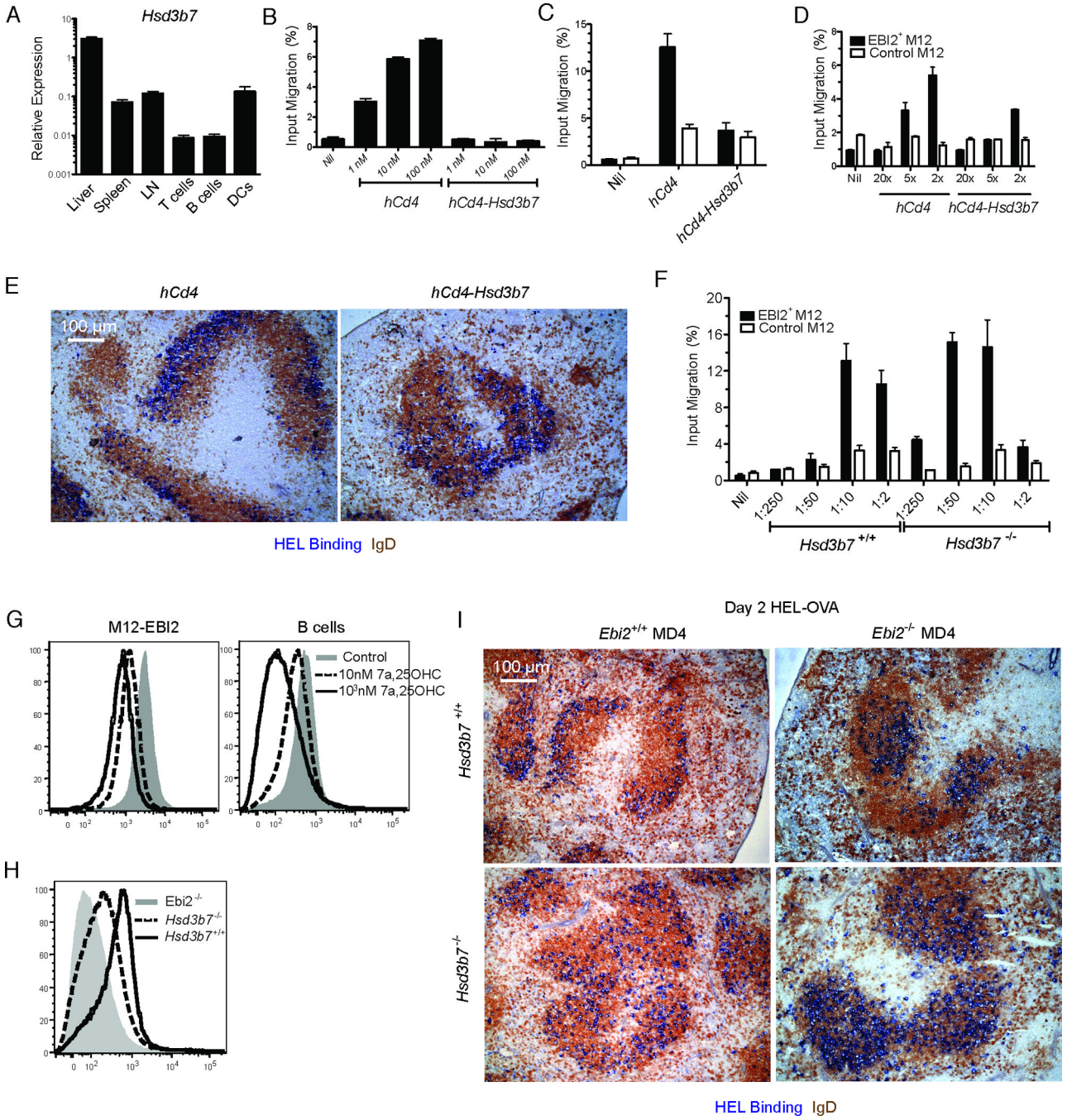

Figure 2. HSD3B7 degrades EBI2-ligand and is required for activated B cell positioning

(A) Quantitative PCR analysis of HSD3B7 transcript abundance in the indicated tissues or cell preparations, relative to HPRT (mean±SE, n=3 mice). T cells were defined as $CD3^+$ cells, B cells as $CD19^+$ cells, DCs as $CD11c^{hi}MHCII^+$ cells. (B) Bioassay measurement of remaining 7α,25-OHC activity following a 6 hr incubation with 293T cells expressing the control (hCD4) vector or HSD3B7 (mean±SE, n=3). (C) Bioassay measurement of EBI2-ligand activity remaining in 10% spleen tissue extract following 6 hr incubation with 293T cells expressing hCD4 or HSD3B7-hCD4 (mean±SE, n=3 mice). (D, E) Mice were reconstituted with BM transduced with an HSD3B7-expressing or control (hCD4) vector. D, Bioassay of spleen extracts (mean±SE, n=3 mice). E, MD4 and OTII splenocytes were

transferred into reconstituted mice and the distribution of MD4 B cells visualized in spleen two days after HEL-OVA immunization. (F) Bioassay of titrated dilutions of spleen extracts from *Hsd3b7*$^{-/-}$ or wild-type animals (mean±SE, n=4 mice). (G) EBI2 surface expression on splenic follicular B cells from *Ebi2*$^{-/-}$, *Hsd3b7*$^{+/+}$ and *Hsd3b7*$^{-/-}$ mice. (H) EBI2 surface expression on M12 cells expressing EBI2-IRES-GFP and splenic B cells, following 35 min incubation with the indicated amounts of 7α,25-OHC or diluted DMSO control. (I) Spleen sections from the indicated mice two days after HEL-OVA immunization. Transferred MD4 B cells were detected by HEL binding (blue) and endogenous B cells with anti-IgD (brown). Data in E-I are each representative of at least 3 experiments.

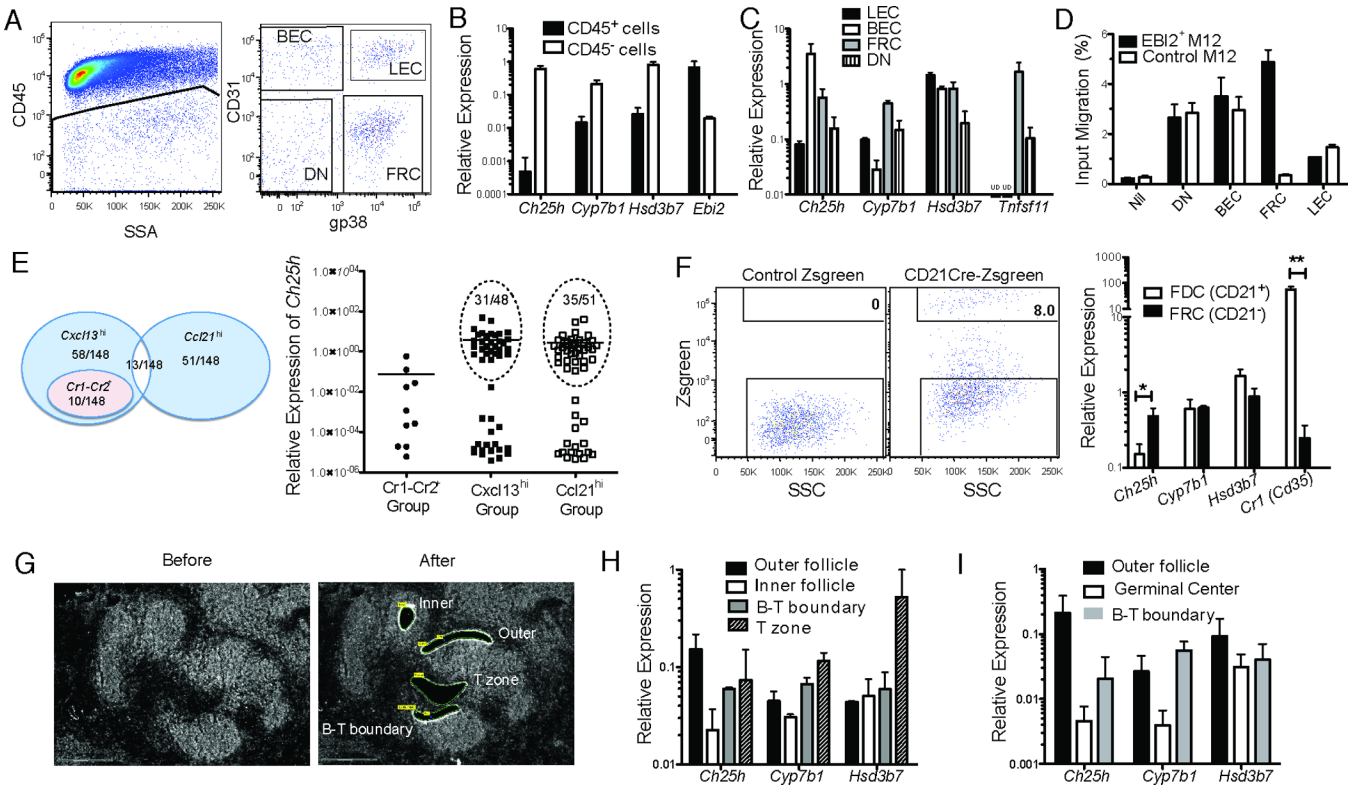

Figure 3. Differential CH25H, CYP7B1, and HSD3B7 expression in lymphoid compartments

(A) Flow cytometric analysis of digested LNs cells showing markers used to identify stromal cell populations. (B, C) Quantitative RT-PCR analysis of total $CD45^+$ and $CD45^-$ cells (B) and stromal cell subsets (C) for the indicated genes, relative to HPRT. Bars indicate mean±SE of samples from 3 independent experiments. (D) Bioassay of supernatant from sorted cells after overnight culture. Bars indicate mean±SE for triplicate wells. One representative of 3 experiments is shown. (E) Quantitative RT-PCR analysis of CH25H transcript relative to HPRT. Data from 148 single-cell analyses are combined from two replicated experiments. Sorted cells were $gp38^+CD31^-$ FRCs identified as in A. Venn diagram shows the number of cells positive for CXCL13, CCL21 and CR1-CR2 transcripts and the overlap in their expression. 16 of the 148 cells were negative for all 3 transcripts. Graph shows the relative expression of CH25H compared to HPRT in cells positive for the indicated transcript. Lines indicate means and dashed circles show the number of cells expressing high amounts of *Ch25h*. (F) Quantitative RT-PCR analysis of CD21-Zsgreen positive or negative $gp38^+CD31^-$ FRCs for the indicated genes relative to HPRT. Bars indicate mean±SE of 4 samples from different experiments. (G–I) Analysis of CH25H, CYP7B1, and HSD3B7 mRNA expression in spleen by laser-capture microdissection and quantitative RT-PCR. G, a representative picture of different lymphoid compartments identified by anti-IgD staining, before and after laser capture. (H and I) Quantitative RT-PCR analysis of CH25H, CYP7B1, and HSD3B7 mRNA in (F) unimmunized and (G) day 7 SRBC-immunized splenic tissues. Data in H and I each show mean±SE for 3 independent capture experiments. * represents $P<0.05$, ** represents $P<0.01$.

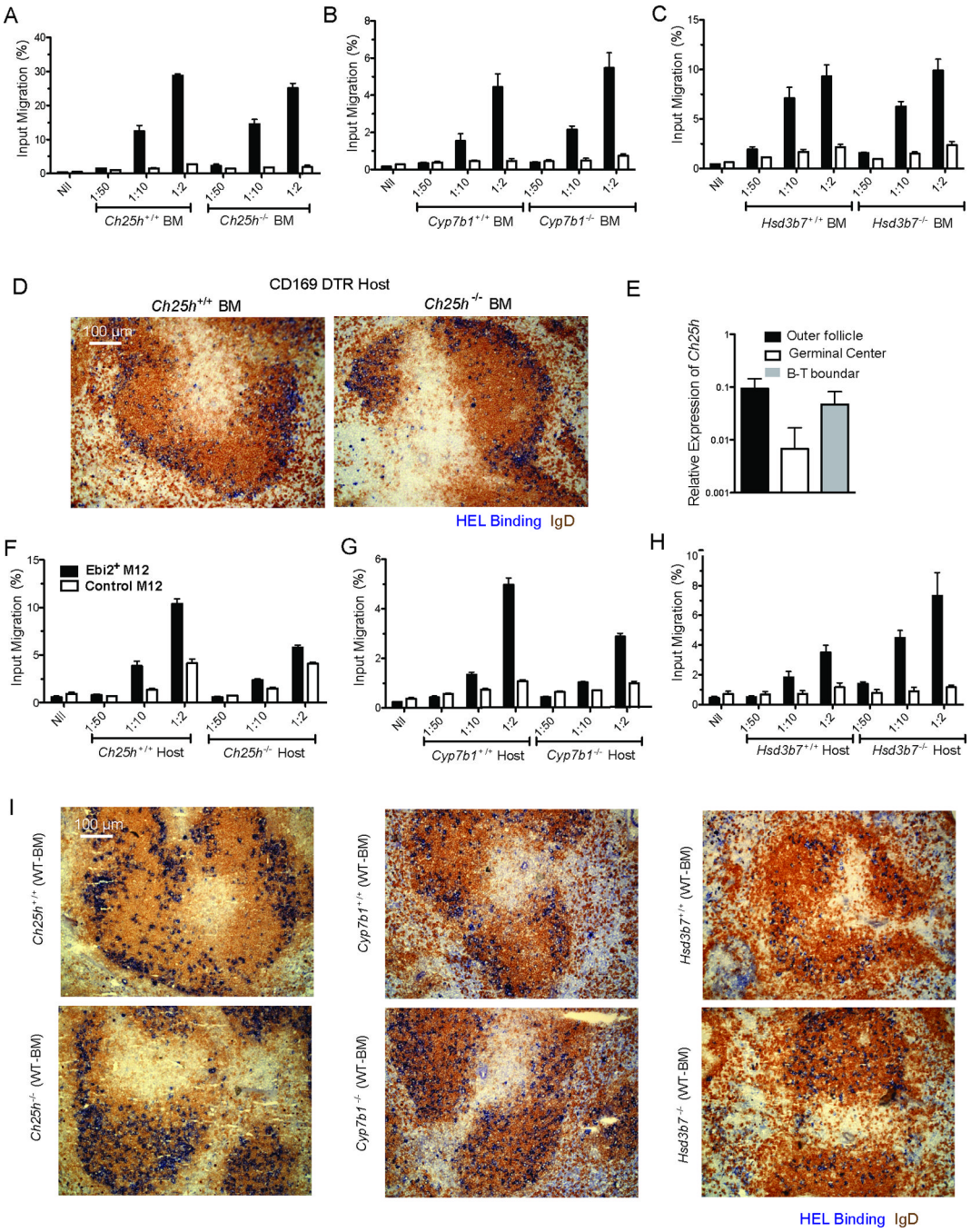

Figure 4. Stromal cells, rather than BM-derived cells, are an important source of 7α,25-OHC for B cell positioning

(A–C) Bioassay of titrated dilutions of splenic tissue extracts from wild-type animals reconstituted with BM cells from *Ch25h*$^{-/-}$, *Cyp7b1*$^{-/-}$, *Hsd3b7*$^{-/-}$ or littermate controls (mean±SE, n=4 mice, one representative of two experiments). (D, E) CD169^{DTR} recipients were reconstituted with BM cells from *Ch25h*$^{-/-}$ or wild-type mice. D, splenic sections from the indicated mice transferred with MD4 B cells and OTII T cells and immunized with HEL-OVA two days before analysis. One representative of at least 3 experiments is shown. E, quantitative RT-PCR analysis of CH25H mRNA (mean±SE, n=3 experiments) in laser capture micro-dissected SRBC-immunized GC-containing splenic tissues. (F, H) Bioassay

of titrated dilutions of splenic tissue extracts from *Ch25h*$^{-/-}$, *Cyp7b1*$^{-/-}$, *Hsd3b7*$^{-/-}$ or their littermate control mice reconstituted with wild-type BM cells (mean±SE, n=4 mice). (I) Spleen sections from the indicated mice that received MD4 B cells and OTII T cells and then were immunized with HEL-OVA 2 days before analysis. One representative of at least 3 replicated experiments is shown.

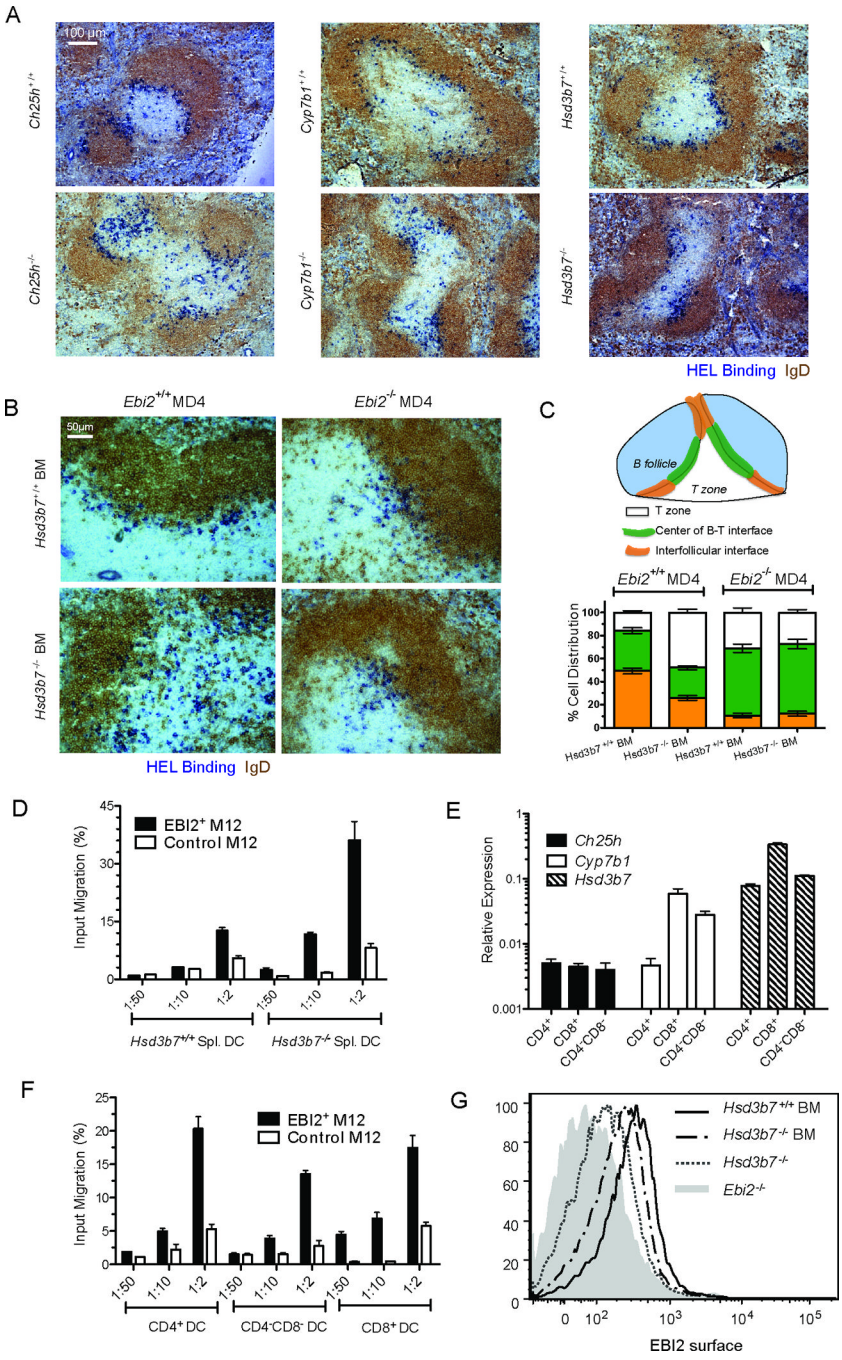

Figure 5. Hematopoietic cells help maintain the T zone as an EBI2-ligand-low environment

(A) Splenic sections from the indicated mice that had received wild-type MD4 B cells, 10 hr after HEL immunization. (B) Splenic sections from wild-type mice reconstituted with *Hsd3b7*$^{-/-}$ or wild-type BM and that received wild-type MD4 cells or *Ebi2*$^{-/-}$ MD4 cells the day before and were immunized with HEL 10 hr before analysis. One representative picture of 4 replicated experiments. (C) Fraction of MD4 cells in T zone, center of B-T interface, and interfollicular interface in the indicated mice. The center was determined as the middle 50% of the B-T interface. The width of the interface is defined as 25% of the follicle diameter. Bars indicated mean±SE, n=15–20 individual follicles from 4–6 different experiments. (D) Bioassay of culture supernatants from FACS-sorted *Hsd3b7*$^{-/-}$ or wild-

type splenic CD11c^{hi}MHCII^{+} DCs (mean±SE, n=3 independent experiments). (E) Quantitative PCR analysis of CH25H, CYP7B1, and HSD3B7 transcript abundance in the sorted DC sub-populations, relative to HPRT (mean±SE, n=4 independent experiments). (F) Bioassay of culture supernatants from DC subpopulations in *Hsd3b7*$^{-/-}$ mice (mean±SE, n=3 different sorting samples). (G) EBI2 surface expression on splenic CD4^{+} T cells from WT recipients reconstituted with *Hsd3b7*$^{-/-}$ or *Hsd3b7*$^{+/+}$ BM or from *a Hsd3b7*$^{-/-}$ mouse. Cells from an *Ebi2*$^{-/-}$ mouse are included as a staining control. One representative of 5 pairs of chimeric mice is shown.

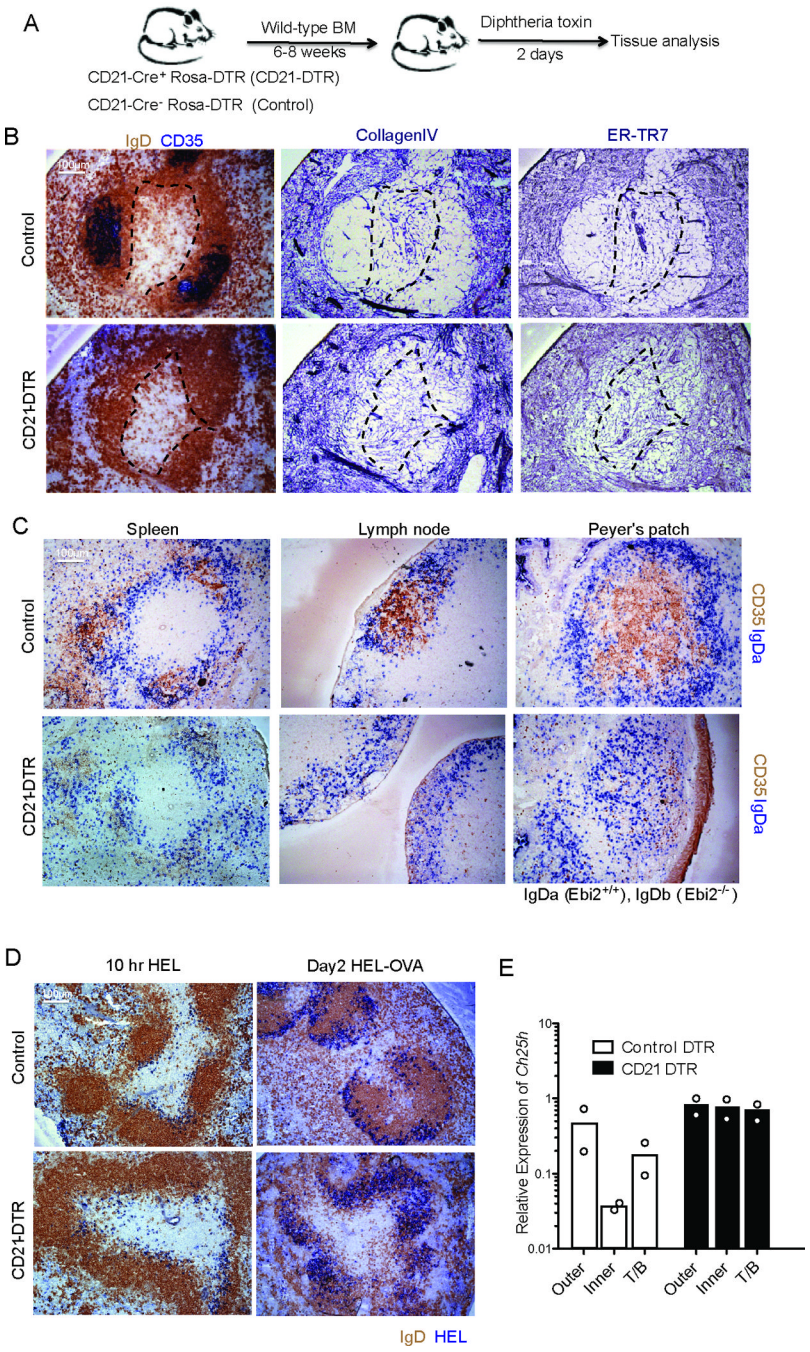

Figure 6. FDCs establish an EBI2-ligand-low environment in the follicle interior

(A, B) ROSA^{DTR+}CD21-Cre^{+} mice that express the DTR in CD21^{+} cells or ROSA^{DTR+}CD21-Cre^{-} control mice were reconstituted with wild-type BM, and the chimeric mice (CD21-DTR or control chimeras) were DTx treated and analyzed 2 days later. A, experimental scheme. B, representative splenic sections with IgD (brown) and CD35, Collagen IV or ER-TR7 (blue) staining. Dashed black lines indicate B-T zone boundary, determined based on IgD stain. (C) CD21-DTR chimeras with mixed Igh^{a} (WT) and Igh^{b} (*Ebi2*$^{-/-}$) were DTx treated 2 days before analysis of spleen, LN, and Peyer's patch sections. (D) Splenic section of DTx-treated CD21-DTR chimeras,10 hr after HEL (left panel) or 2 days after HEL-OVA (right panel) immunization. One representative of 3

replicated experiments is shown. (E) Analysis of CH25H mRNA expression in spleen tissue from FDC-ablated or control mice by laser-capture microdissection and quantitative RT-PCR. Data show the mean of two different capture experiments and are representative of two further experiments.

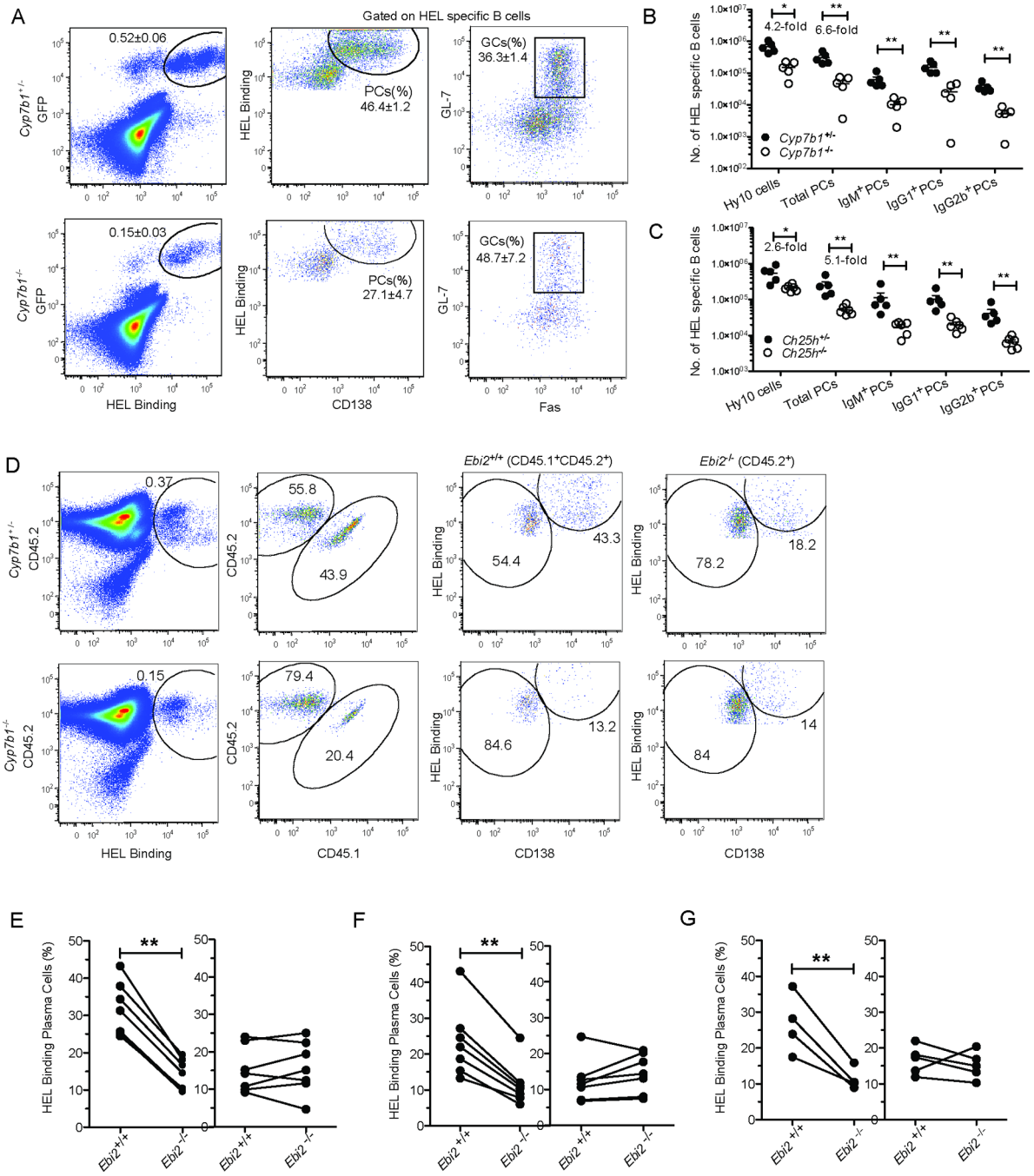

Figure 7. Lack of CYP7B1, CH25H and HSD3B7 results in diminished plasma cell Responses

(A) Plasma cell response in *Cyp7b1*$^{-/-}$ or littermate control mice receiving Hy10 cells at day 5 after immunization with SRBCs conjugated with HEL$^{2\times}$. Percentage of HEL-binding Hy10 B cells, HEL-binding^{hi}CD138^{hi} PCs and HEL-binding^{hi}Fas^{+}GL7^{+} GC cells amongst total splenocytes are shown as mean±SE (n=5 mice). (B, C) Numbers of HEL-binding B cells, total plasma cells, and plasma cells in different Ig isotypes (mean±SE, n=5 mice) in *Cyp7b1*$^{-/-}$, *Ch25h*$^{-/-}$ or littermate control mice. (D, E, F, G) Plasma cell response in *Cyp7b1*$^{-/-}$, *Ch25h*$^{-/-}$, *Hsd3b7*$^{-/-}$ or littermate control mice that received mixed *Ebi2*$^{-/-}$ Hy10 (CD45.1^{+}) and wild-type Hy10 (CD45.1^{+}CD45.2^{+}) cells and were immunized with SRBCs conjugated with HEL$^{2\times}$. D, representative plasma cell gates of *Cyp7b1*$^{-/-}$ or

littermate control recipients; E-G, percentage of plasma cells in *Cyp7b1*$^{-/-}$, *Ch25h*$^{-/-}$, *Hsd3b7*$^{-/-}$ or littermate control mice (mean±SE, n=4–8). * represents P<0.05, ** represents *P*<0.01